ORIGINAL ARTICLE

Anthropogenic subsidence in the Mexicali Valley, Baja California, Mexico, and slip on the Saltillo fault

Ewa Glowacka · Olga Sarychikhina ·
Francisco Suárez · F. Alejandro Nava ·
Robert Mellors

Abstract Deep fluid extraction in the Cerro Prieto geo- thermal field (CPGF) has caused subsidence and induced slip on tectonic faults in the Mexicali Valley (Baja Cali- fornia, Mexico). The Mexicali Valley is located in the southern part of the Salton Trough, at the boundary between the Pacific and North American plates. The Valley is characterized by being a zone of continuous tectonic deformation, geothermal activity, and seismicity. Within the Cerro Prieto pull-apart basin, seismicity is concentrated mainly in swarms, while strong earthquakes have occurred in the Imperial and Cerro Prieto transform faults, that are the eastern and western bound of the basin. Since 1973, fluid extraction at the CPGF has influenced deformation in the area, accelerating the subsidence and causing rupture (frequently as vertical slip or creep) on the surface traces of tectonic faults. Both subsidence and fault slip are causing damage to infrastructure like roads, railroad tracks, irriga- tion channels, and agricultural fields. Currently, accelerated extraction in the eastern part of CPGF has shifted eastwards the area of most pronounced subsidence rate; this accele- rated subsidence can be observed at the Saltillo fault, a southern branch of the Imperial fault in the Mexicali Valley. Published leveling data, together with field data from geo- logical surveys, geotechnical instruments, and new InSAR images were used to model the observed deformation in the area in terms of fluid extraction. Since the electricity

E. Glowacka (✉) · O. Sarychikhina · F. A. Nava
Department of Seismology, CICESE, Ensenada, Mexico
e-mail: glowacka@cicese.mx

F. Suárez
Department of Geology, CICESE, Ensenada, Mexico

R. Mellors
Department of Geology, SDSU, San Diego, USA

production in the CPGF is an indispensable part of Baja California economy, extraction is sure to continue and may probably increase, so that the problem of damages caused by subsidence will likely increase in the future.

Introduction

The Mexicali and Imperial Valleys are part of the Salton Trough tectonic province, which is located at the boundary between the Pacific and the North American plates. The Salton Trough (Fig. 1) is the connection between the Gulf of California depression to the South and the transform boundary of the San Andreas fault system to the North, and includes: the Cerro Prieto, Imperial, San Jacinto and Southern San Andreas right-lateral transform faults, as well as the Brawley, Cerro Prieto, and Heber, step-to- the-right, extensional, basins (Magistrale 2002).

A schematic idea of the geological and tectonic situation in the area of the Cerro Prieto basin is presented in Figs. 2 and 3. The basement on the western side of the basin is composed of Cretaceous granites. At the center, the domi- nant rock is intrusive mafic, and on the eastern side the basement is a Paleozoic Metamorphic slate (Lira 2005). Tertiary extension caused thinning of the crust and devel- opment of the basin characterized by fast subsidence followed by high heat flow and rapid sedimentation. Over- lying the granitic basement rests a thick sequence of gray shale with interbeded sandstone, with an average thickness of 2,700 m. Over the gray shale there is a sequence of Tertiary brown-shale and mudstone (Fig. 3). The entire sequence is covered by continental unconsolidated clastic
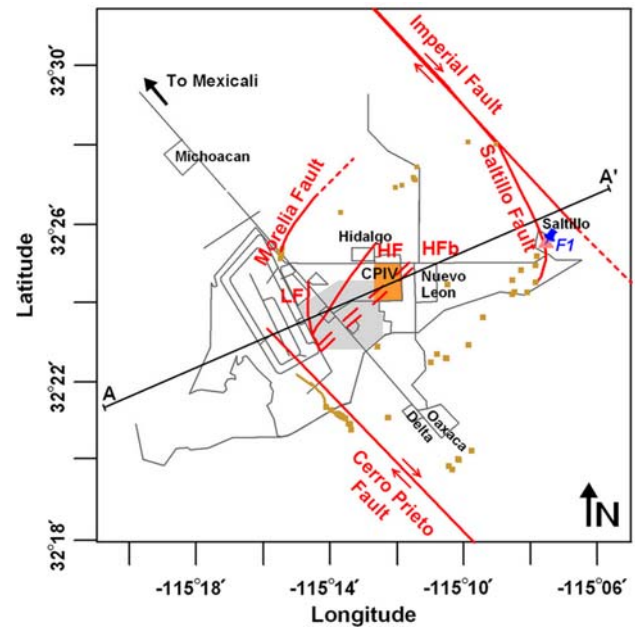
🖄 Springer
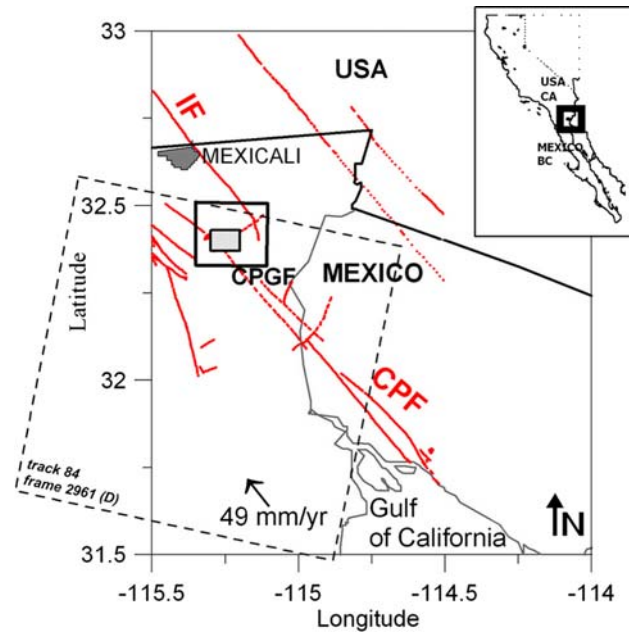
Fig. 1 Location map. *CPGF* Cerro Prieto geothermal field (*small, gray rectangle*), *large rectangle* study area, *red lines* faults: *IF* imperial fault, *CPF* Cerro Prieto fault. *Dotted rectangle* spatial coverage of Envisat images

Fig. 2 Details of studied area. F̄1location of photograph shown in Fig. 6. *Triangle* crackmeter. *Red lines* indicate faults: *LF–L* fault, *HF–H* fault on the surface, *HFb–H* fault on the intersection with reservoir. *Solid, brown squares* are sites of superficial evidence of subsidence. A *gray polygon* indicates extraction area before year 2000, an *orange rectangle* indicates the area of CPIV wells. Modified from Glowacka et al. (1999), and Suarez-Vidal et al. (2008)

sediments, supplied by the Colorado River and by the westerly alluvial fans from the Cucapah Ranges, which include gravel, sands, and clays with an average thickness of 2,500 m (Lira 2005). Due to local tectonics the sedimentary sequence is dissected, displaced and tilted by normal faults. Thick sedimentary sequences, high heat flow, active faults, and water from the Colorado River created perfect conditions to produce geothermal steam.

Fluid extraction for electricity production began in the Cerro Prieto geothermal field (CPGF) in 1973 from depths of 1,500–3,000 m. Re-injection of residual water began in 1989, and currently about of 20% of the extracted water is being reinjected at 500–2,600 m depths. The geothermal field is operated by the Mexican Federal Electricity Commission (Comisión Federal de Electricidad, CFE). At present, the CPGF has a 720 MW capacity and is the world's second largest geothermal field. Cerro Prieto is a high-temperature, fluid-dominated field, contained within sedimentary rocks. The geothermal fluid, with a temperature of 260–350°C, is extracted from gray shales, and is isolated from the unconsolidated rock by a layers of mudstone and brown shales which constitute the cap-rock (CFE 2006). The extracted volume increased from 14 million tons in 1974 to 72 million tons in 2005.

The CPGF reservoir is characterized by having "leaky" boundaries, where the hot geothermal fluids exist in dynamic equilibrium with much cooler waters (Truesdell and Lippmann 1990). It is generally accepted that the field

is recharged from two sources, a deep one, to the east, that supplies hot water, and a second source which contributes cold water from shallow aquifers, located to the east, west, and south, fed by the Colorado River (Truesdell et al. 1998).

From the analysis of the leveling surveys done in the area of CPGF and the Mexicali Valley since 1977, Glowacka et al. (1999) noticed that, for the period 1977–1997, the subsidence rate at the center of the field increased after each steam extraction increase. The area of maximum subsidence rate, 12 cm/year, coincided with that where the extraction wells were located, and this subsidence rate was too high to be caused by tectonic activity alone. These facts suggested that subsidence in the CPGF was caused mainly by fluid extraction. Subsidence at CPGF was also measured by Synthetic Aperture Radar (SAR) interferometry by Carnec and Fabriol (1999) and Hanssen (2001), using ERS1/2 images acquired in 1993–1997 and 1995–1997 periods, respectively, and was interpreted as being produced by geothermal fluid extraction.

Surface deformation is an expected consequence of the extraction of geothermal fluids. Surface subsidence rates of dozens of centimeters per year have been measured across several major geothermal fields, e.g., Wairakei, New Zealand (Allis et al. 1998) and Geysers, USA (Mossop and Segall 1997).

To quantitatively evaluate the tectonic component of the subsidence recorded in the Mexicali Valley, Sarychikhina
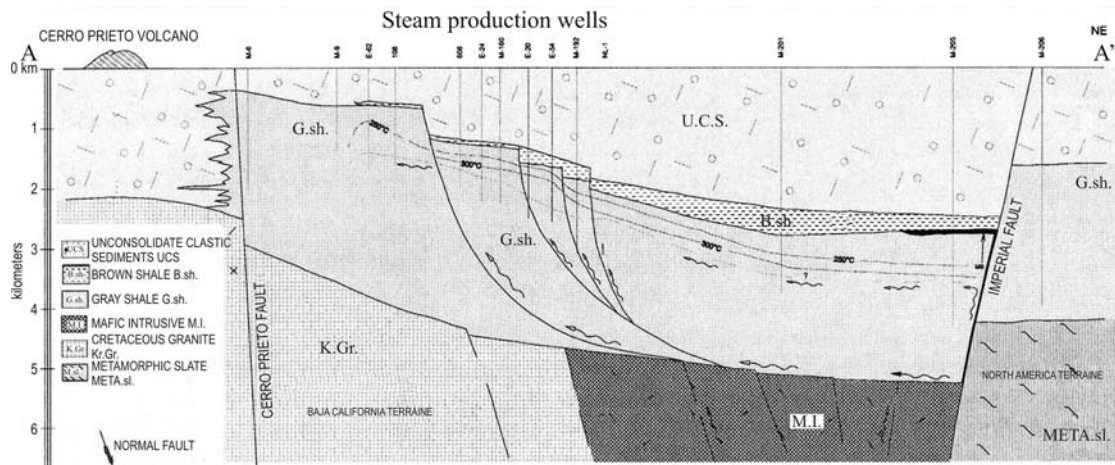
Fig. 3 Geological section along AA′ of Fig. 2 (modified from Lira 2005)

(2003) and Glowacka et al. (2005) modeled the elastic deformation caused in the pull-apart basin by the tectonic extension between the Imperial and Cerro Prieto strike slip, right lateral faults, using slip rates determined by GPS measurements of over the plate boundary (Bennett et al. 1996). This modeling estimated a maximum subsidence rate of 0.45 cm/year, over an area coinciding with that of the CPGF, and taking into account compaction and isostasy, this rate could attain ∼0.60 cm/year. The estimated tectonic subsidence is of the order of those calculated for nearby areas using other methods: 0.16 cm/year for Laguna Salada, 20 km west of Mexicali (Contreras et al. 2002), and 0.55 cm/year for the Vallecito–Fish Creek basin 50 km north of Mexicali (Johnson et al. 1983).

Thus, the estimated tectonic subsidence rate in the area of CPGF is of the order of only 4–5% of the total 12 cm/year measured rate; leaving some 95% to anthropogenic causes. According to Camacho Ibarra (2006), 82–90% of the observed subsidence in this region is anthropogenic.

Although the extension and the shape of subsidence zone in the Mexicali Valley suggest that these parameters define the pull-apart basin originally controlled by tectonics, the current subsidence rate is mainly related to fluid extraction.

Tectonic faults play an important role in feeding and constraining the geothermal reservoirs. The role of the faults located in the extraction zone was analyzed by Lippmann et al. (1991). According to these authors, faults H and L (Fig. 4) function as conduits for hot and cold water recharging, and as boundaries between reservoirs α, β and γ. As a consequence of fluid extraction and the corresponding pressure drop in the geothermal reservoir, the cold water from a shallow aquifer recharges the geothermal fluid (Lippmann et al. 1991).

Field observations done since the 1980s show that the observed subsidence is not continuous in space and is characterized by abrupt vertical displacements along the known traces of the Imperial and Cerro Prieto faults. Analysis of the extension, amplitude, and time behavior of the slip (relative displacement across the fault) on the Imperial and Cerro Prieto faults, which bound the Cerro Prieto pull-apart basin from the NE and the SW (Glowacka et al. 1999, 2005), suggested that these faults constitute a boundary of the subsided area, and probably are a groundwater barrier.

The objective of the present work is to use existing field (geodetic, geotectonic and geotechnical) data together with two-pass differential Interferometric Synthetic Aperture Radar (InSAR) technique to model the current spatio-temporal evolution of the surface deformation in the CPGF area.

Subsidence

Since 1962 (Velasco 1963), leveling surveys in the CPGF and the neighboring area were done, mainly by CFE, every few years, with different precisions, coverage, and densities of precise leveling; GPS surveys have also been carried out since the 1990s. Glowacka et al. (1999, 2005) used the most complete set of data recorded during the 1994–1997 period by CFE (Lira and Arellano 1997) and CICESE, to analyze the magnitude and shape of the deformation caused by fluid extraction. Their results are shown in Fig. 4, where the dominant feature is an elliptical area with the highest subsidence rate, oriented NE–SW. The shape of the area agrees with the boundaries of the geothermal anomaly and is within the area of tectonic subsidence. The maximum subsidence rate ∼12 cm/year was located at the center of the extraction zone; while a second, local maximum with subsidence rate ∼9 cm/year was located to the NE of the field. Since the second maximum is located outside the extraction area it was interpreted as an area of fluid recharging.

This rapid subsidence and the associated fault slip (more than 2 m accumulated since the 1970s) in an otherwise flat
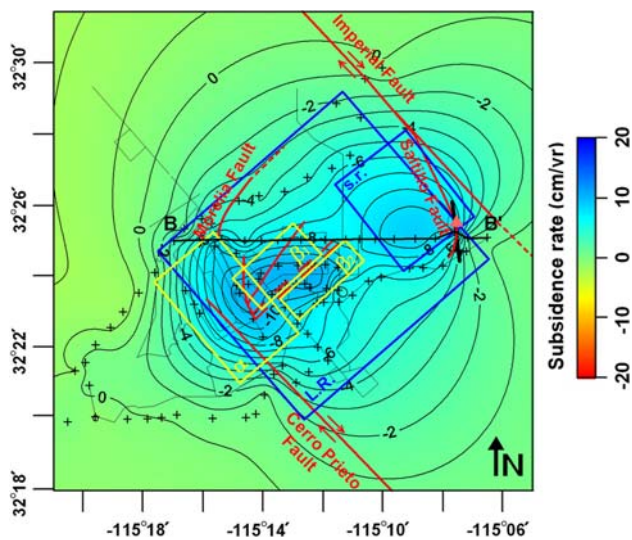
Fig. 4 Subsidence rate for 1994–1997 in cm/year. *Red lines* indicate faults (see Fig. 2 for names). *Yellow* and *blue rectangles* represent the surface projection of modeled geothermal reservoirs and modeled aquifers which recharge water to the field, respectively (modified from Glowacka et al. 2005). The *black line* is the surface trace of the modeled Saltillo fault (SF)

region, cause damage to roads, railroad tracks and irrigation systems (both major and local irrigation channels). The step in ground level causes problems to farming fields irrigated from channels: in the subsiding side it causes a health hazard because it is not possible to drain waste agriculture water from the subsidence basin; on the upper side, it causes economic problems in farms which do not receive enough water for agricultural production. It is also a source of hazard because, in the event of even a moderate earthquake, the shaking could cause damage with resulting floods if the one of the, currently barely functional, main irrigation channels gets broken.

Some of the features observed on the surface related to the subsidence, and damage caused by subsidence to local infrastructure, have been described by González et al. (1998), Glowacka et al. (2006) and Suarez-Vidal et al. (2008). The name Imperial Fault was used for Saltillo Fault until distinction between the two branches was made by Suarez-Vidal et al. (2008).

To evaluate the elastic deformation caused by fluid extraction, when the depth of the subsidence source is large compared with the dimension of the affected area on the surface, mathematical models used for volcanology and hydrofracturing can be used. The one most commonly used is Mogi's (1958) model of a spherical hydrostatic pressure source imbedded in an elastic half-space. This model was used by Mossop and Segall (1997) to model subsidence in the Geysers geothermal field, and by Carnec and Fabriol (1999) and Hanssen (2001) to model subsidence in the CPGF. The model of deflation of a triaxial ellipsoidal

cavity in an elastic half-space (Davis 1986) was used for subsidence modeling in the Coso geothermal field (Fialko and Simons 2000). The subsidence induced by fluid extraction was evaluated by Segall (1989) using a poro-elastic model of an axisymmetric reservoir. All these models have some kind of symmetry: three- or two-dimensional, which does not seem appropriate for the CPGF. Because the CPGF reservoirs are located in sedimentary layers and bounded by faults, the decision was made to use the mathematical model of rectangular tension fractures (Yang and Davis 1986) as the one which best represents the geometry of reservoirs.

Thus, anthropogenic subsidence was evaluated using a model of rectangular tensional fractures, based on the hydrological model of CPGF proposed by Lippmann et al. (1991), together with the Coulomb 2.0 software (King et al. 1994; Toda et al. 1998); model parameters were adjusted by trial and error. The final model (Sarychikhina 2003; Glowacka et al. 2005) consists of five tensional rectangular cracks which represent three geothermal reservoirs, located in the CPGF production zone (α, β_1 and β_2), a shallow recharge aquifer that covers a wide zone between two major faults (L.R) and a local recharge aquifer located between the CPGF production zone and the Saltillo fault (s.r) (Fig. 4; Table 1).

To evaluate the quality of modeling, residuals from measured minus modeled subsidence rates were plotted as dotted blue line along line BB′ in Fig. 5. One can see that very high values of residuals are present close to the Saltillo fault, which constitutes the eastern boundary of the subsidence region and presents well documented slip (described below). To avoid these high residuals it is necessary to include in the modeling a correction for vertical displacement on this fault. The correction was made by including a shear fracture representing a normal fault (west side down). The modeling was done using the Coulomb 2.0 software and fitting the parameters by trial and

Table 1 Model parameters: z is the depth to the center of fracture or fault

Fracture/fault	Parameters				
	z (m)	p (cm/year)	Azim (°)	Ang	Color (Fig. 4)
α	1,100	−5.0	140	1	Yellow
β_1	2,100	−10.0	138	4	Yellow
β_2	2,250	−12.0	138	4	Yellow
s.r.	1,500	−7.9	142	7	Blue
L. R.	996	−4.0	139	1	Blue
SF	600	−7.0	173	−70	Black

p is the yearly rate of aperture of fractures or fault slip; reverse slip is positive, *azim* is the azimuth of fracture/fault, *ang* is the dip angle of the fracture or fault

error, to minimize the residuals. The parameter values: length 3 km, width 1.2 km, displacement rate 7 cm/year, and dip 70° (Table 1), reduce the residuals as shown by the solid green line in Fig. 5. While a normal fault is needed in the modeling, it should be pointed out that the parameter set which satisfied our problem is not unique, so that these values should only be used as rough estimates of the true values. Since the vertical motion on the Saltillo is mainly due to fluid extraction, it is not unreasonable to suppose the fault to reach to, or close to, the depth of the s.r. fracture 1.5 km, which implies a fault width ~1.6 km.

Field data

The effects of subsidence are clearly seen along the faults that bound the subsidence zone. The Colorado River was the principal source of the very high sedimentation in the Mexicali valley that kept the active faults covered, but since it was dammed in 1934, sedimentation from this source stopped (Suarez-Vidal et al. 2008) and, since then, surface traces of active faults have appeared in places when

Table 2 Interferometric pair used in this study

Satellite	Track_frame	Image 1	Image 2	$B\perp$ (m)	B_{temp} (days)
ENVISAT	84_2961 (D)	2005/12/04	2006/02/12	−300	70

D indicates a descending orbit, $B\perp$ is the perpendicular baseline, B_{temp} is the time span between satellite passes
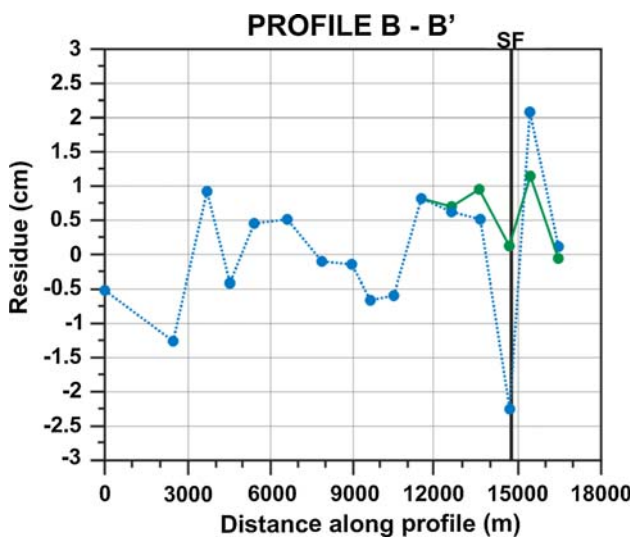
Fig. 5 Residuals from the B–B′ profile of Fig. 4, *dotted blue* difference between observed and modeled deformation with tensile fracture only, and *solid green* residuals after including vertical displacement on the Saltillo fault (the fault location is indicated by the *black vertical line*)

there is no agricultural activity. These surface breaks have been studied and published by González et al. (1998), Glowacka et al. (1999), and Lira (2005), and summarized recently by Suarez-Vidal et al. (2008).

Detailed field mapping done during 2005–2007 in the vicinity of the CPGF shows many fractures, fissures, collapse features, small grabens and vertical displacements. These features were documented, measured, and photographed; their azimuths were determined, and, where possible, they were associated with known tectonic faults. Some of the measurements were published in Glowacka et al. (2006) and Suarez-Vidal et al. (2008). The area affected by visible fractures, documented since the 1980s, is shown in Fig. 2. The affected area is localized between the Cerro Prieto and Morelia faults to the NW, and the Imperial and Saltillo faults to the SE, which, according to Suarez-Vidal et al. (2008), limit the Cerro Prieto pull apart basin. This affected area is larger than that of the CPGF, where the extraction wells are located, and extends eastwards to the Saltillo fault (Figs. 2, 6).

Since 1996, geotechnical instruments have been operated by CICESE in the Mexicali valley, for continuous recording of deformation phenomena. The vertical displacement at the southernmost part of the Saltillo fault has been measured on a continuous basis since February 1996 by a crackmeter (Geokon Vibrating Wire, model 8001, high range, 0.1 mm precision, extensometer), installed in Ejido Saltillo (Glowacka 1996; Nava and Glowacka 1999) which samples at intervals of 10 or 20 min. The 3 m long crackmeter spans the fault in a plane perpendicular to it (Fig. 7). The crackmeter extends from a base anchored to the eastern (higher) side of the fault to a base within a small graben in the western side.


Fig. 6 Photograph of site F1 (Fig. 2) showing the Saltillo fault where the crackmeter is installed as seen from the S. This place was flat in the beginning of the 1970s

Fig. 7 Schematic section of crackmeter installation
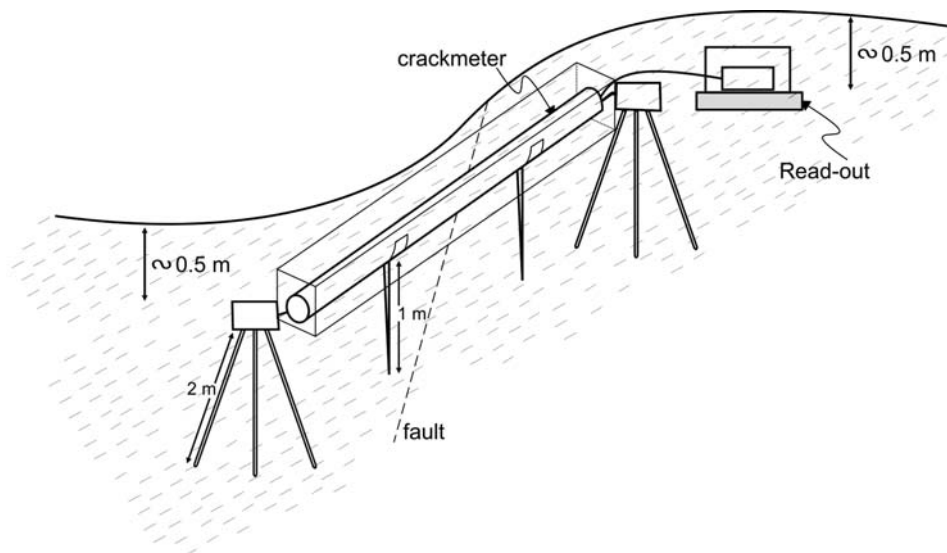
Fig. 8 Vertical displacement versus time, for 1996–2007, in mm/year; note change in slope during the second half of 2003. *Inset* is a close-up of the 1998 slip event
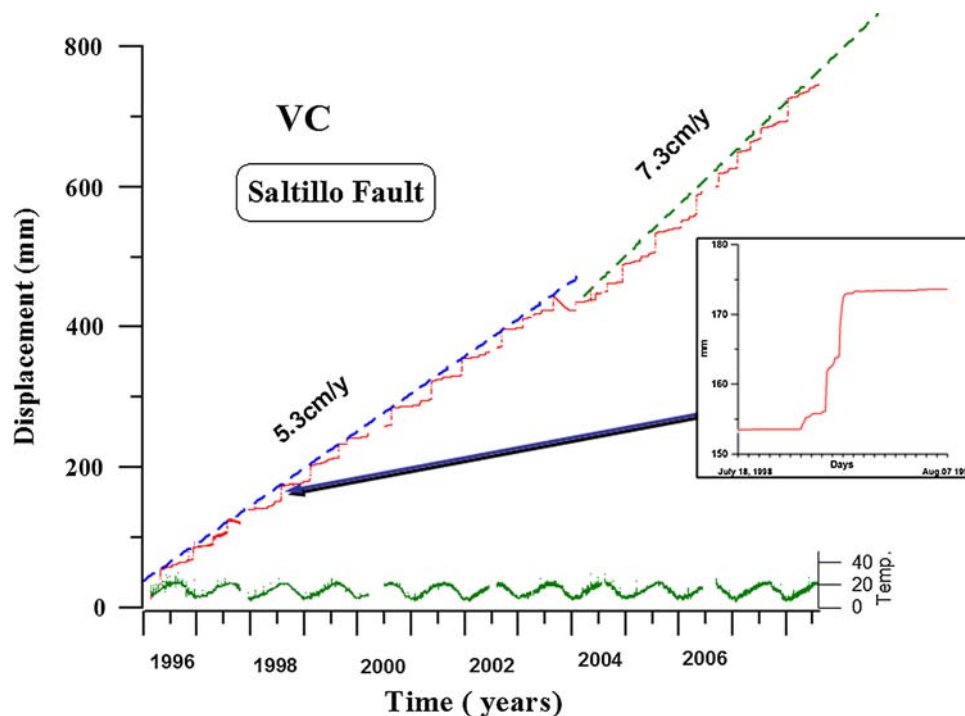

In Fig. 8, it can be seen that the vertical slip on the Saltillo fault is not continuous, but occurs mainly in steps (episodic slip or creep events), separated by months of very slow monotonic displacement; large events account for about half of the vertical displacement. Creep events have amplitudes of 1–3 cm and durations of 1–3 days. The displacement curve, together with the fitted (dashed) tangential lines, also show that vertical slip is slip-predictable for large slip events, and is aseismic (Glowacka et al. 2001). Quite conspicuously, the measured slip rates (fitted line slopes) for the Saltillo fault changed from 5.3 to

7.3 cm/year, over some time during the second half of 2003; we will come back to this slope change later on.

InSAR data

Interferometric synthetic aperture radar (InSAR), is a radar technique used in geodesy and remote sensing. This geodetic method uses two or more synthetic aperture radar (SAR) images to generate maps of surface deformation or digital elevation, using differences in the phase of the
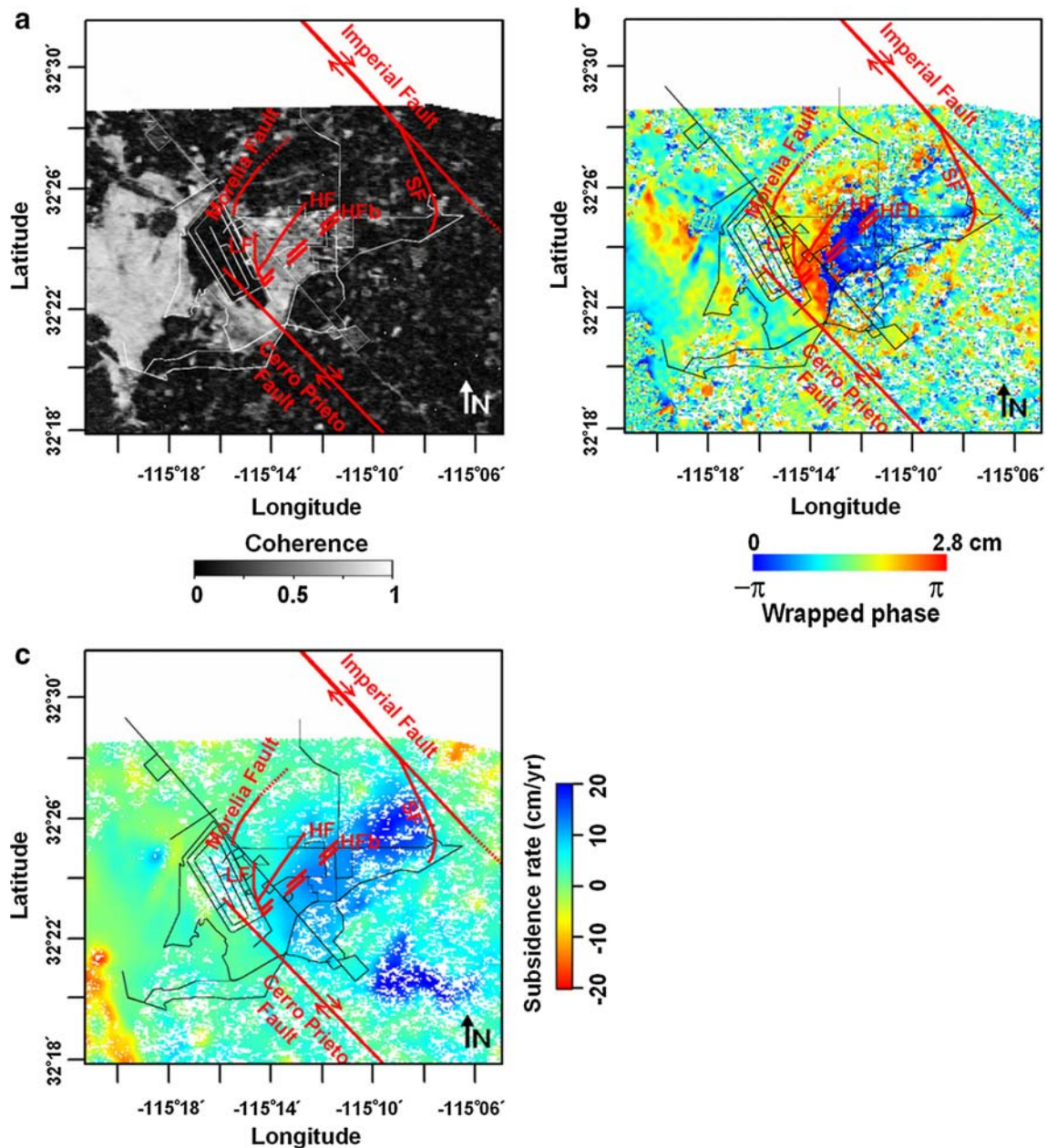
Fig. 9 Geocoded InSAR images: coherence (**a**), wrapped phase (**b**), and surface vertical displacement (per year) (**c**), respectively, of the interferometric pair listed in Table 2. The area of low coherence (<0.1) is masked in **b**, **c**

waves returning to the satellite (Hanssen 2001). The technique can potentially measure centimeter-scale changes in deformation over time spans of days to years. It has applications for geophysical monitoring of natural and induced hazards, for example earthquakes, volcanoes, landslides, subsidence and structural stability.

Synthetic Aperture Radar images (single-look complex) from the European Space Agency (ESA), were used to generate interferograms, using the Doris InSAR processing software (Kampes et al. 2003) and precise satellite orbits from Delft University (Scharoo and Visser 1998). The

topographic effects were removed from the interferograms, using the Shuttle Radar Topography Mission (SRTM) 3-arcsec digital elevation model. Unwrapping was performed using the SNAPHU software (Chen and Zebker 2001). Preliminary results of InSAR data analysis for the study area over the period 2004–2005 have been presented in Sarychikhina et al. (2007a, b). In this paper we present an analysis of one ENVISAT interferogram, which was selected from 20 interferograms from the period 2004–2006 based on good correlation and lack of obvious atmospheric artifacts. The selected interferogram spans a

35 day period (2004/12/19–2005/01/23) and is from descending track images (track 84, frame 2961). The spatial coverage of this interferogram is presented in Fig. 1.

Geocoded interferometric results for coherence, wrapped phase and vertical displacement rate normalized per year are shown in Fig. 9. The interferogram was spatially low-pass filtered to smooth out image noise and reduce spikes in the data. This filtering was done through a two-dimensional convolution with a 9 by 9 pixels boxcar kernel matrix.

The interferogram has good coherence at the CPGF zone and its surrounding area, and the deformation pattern is clearly visible. High deformation rates define a roughly elliptical area oriented NE–SW, featuring two subsidence basins. The elliptical area, and the two basins coincide with those from the 1994–1997 leveling; but whereas for the older study the highest subsidence rate ($\sim$12 cm/year), was east of the evaporation basin at the center of the CPGF, in the present study we find not only that the subsidence rate at this point has increased to $\sim$1.2 cm/month (14 cm/year), but that the highest subsidence rate $\sim$1.7 cm/month (20 cm/year) is found now at the other basin, located to the NE, close to the Saltillo fault in what was previously proposed as a region of recharge.

Discussion

A recapitulation of facts resulting from new field, instrumental and InSAR observations is: The subsidence area is limited by faults, and this phenomenon is mainly seen along the Saltillo fault. During the last few years the subsidence rate increased over all the area, but this increase was significantly larger towards the NE, at the eastern subsidence basin, located outside of CPGF. Slip on the Saltillo fault, which corresponds to about half of the total subsidence, occurs mainly during slip events. The vertical slip rate on the fault increased from 5.3 to 7.3 cm/year around second half of 2003. We will now proceed to interpret and discuss these facts.

Three processes are probably at work to produce the observed fault behavior. According to Sheng and Helm (1998), existing faults often are poorly permeable in the direction perpendicular to the fault, and play the role of a ground water barrier, increasing differential displacement of both sides of the fault. Additionally, the process of fault breaking is accelerated by fluid extraction, when different thicknesses of sediments in both sides of the fault (as seen in Fig. 3) induce differential compaction and, hence, tensional and shear stresses on the ground mass, thus producing ground failures leading to vertical displacement on the faults which limit the affected aquifer (op cit.). Thirdly, a diminution of the normal stresses is to be

expected at the fault, due to extension at the edge of a subsidence basin, which reduces the friction that locks the fault (Segall 1989).

Given the above, the second question is why the slip is episodic. The presence of displacement in form of slip events is probably related to the stick-slip mechanism during a subsiding process. A similar process was suggested, by Pennington et al. (1986), as the cause of seismicity induced by petroleum production. The presence of slip events suggests that the subsidence is a relatively deep phenomenon, and slip events are located between the depth of the seismogenic zone (high normal stresses) and the upper part of the fault, where normal stresses, caused by closing of both aquifers (L.R and s.r), are small enough to allow the slip to be continuous.

The occurrence of aseismic slip events is well documented on active, strike-slip faults in California, and has been observed and documented since the 1960s (e.g. Wesson 1988). Bilham and Behr (1992) analyzed aseismic slip phenomena on the Superstition Hills strike-slip fault, and suggested that stable sliding should extend from the surface to the zone of episodic slip, which ranges from $\sim$300 m to $\sim$3 km depth where the seismogenic zone begins, and the different slip behaviors are due primarily to the lithostatic increase in fault normal stress.

However, seismicity in the Mexicali valley ranges in depth between $\sim$1 km and 15 km, with most earthquakes occurring between 4 and 6 km (Glowacka et al. 1999), near the southern part of Imperial fault (Glowacka et al. 2002) seismicity occurs below the 2 km depth. Near the southern part of the Imperial fault unconsolidated sediments reach depths of $\sim$2.5 km west of the fault (Fig. 3). A depth of $\sim$2.5 km agrees well with the upper limit of seismicity, while the estimated depth of the deep s.r. fracture and width of the SF fault (modeled above) suggest a slightly shallower limit of $\sim$1.5 and $\sim$1.1 km, respectively. Within the uncertainties in these data we speculatively propose the depth range of slip events to be from $\sim$1 to $\sim$2.5 km.

As mentioned above, the main difference between the subsidences measured using InSAR for 2004–2005, and those from the 1994 to 1997 leveling, is that the maximum subsidence rate shifted eastwards from the older part of the CPGF towards the edge of the basin, close to the Saltillo fault. Similar results were obtained for different pairs of SAR images from 2004 to 2005, and were attributed to changes in the spatial distribution of steam extraction (Sarychikhina et al. 2007a, b). In 2000 a new power plant began operating in the newest, eastern part of the CPGF, named Cerro Prieto IV (CPIV), shown in Fig. 2, extracting steam from a depth of around 3.5 km (Ocampo-Diaz 2005).

Talwani and Acree (1984/1985) proposed that seismicity induced by dam filling and fluid injection occurs with a
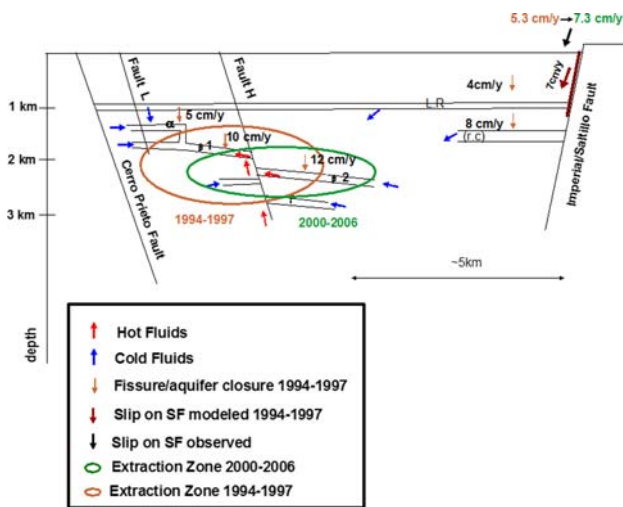
Fig. 10 Schematic section of new hydrological model

time lag related to the distance from the source of the pressure change, by a process of pore pressure diffusion, with a "seismic" hydraulic diffusivity in the range 5×10^3–5×10^5 cm^2/s. To explore whether the subsidence rate change recorded by the crackmeter on the Saltillo fault, that began around mid 2003, could be attributable to the change in production location, we calculated the value of hydraulic diffusivity that could account for the time delay of about 3 years, given that the Saltillo fault is about 5 km to the east of CPIV. We obtained a hydraulic diffusivity of the order of 10^4 cm^2/s, close to the 3×10^4–3×10^5 cm^2/s, determined by Glowacka (1996) for seismicity related to the fluid extraction (pressure decrease) in the CPGF in the same area.

The schematic section of the hydrogeological model presented above, is summarized in the Fig. 10.

Conclusions

Data from leveling and geological surveys, geotechnical instruments and satellite observations, together with model estimates on the active tectonics of the area, indicate that fluid extraction in the CPGF is the major cause of subsidence in the area and this subsidence can influence vertical displacement on the Saltillo fault through several mechanisms.

The distance and time relation between the extraction changes in the CPGF and displacement rate changes on the Saltillo fault suggests that the fault is affected through diffusive transmission of pore pressure changes with a characteristic hydraulic diffusivity.

Since the electricity production at the CPGF is an indispensable part of Baja California economy, economic pressures will surely result in future increased extraction

and consequently, increased subsidence with a higher rate and more extended spatial area.

References

Allis RG, Zhan X, Clotworthy A (1998) Predicting future subsidence at Wairakei field, New Zealand. Geotherm Resour Counc Trans 22:43–47

Bennett RA, Rodi W, Reilinger RE (1996) Global positioning system constrains on fault slip rates in Southern California and Northern Baja, Mexico. J Geophys Res 101(B10):21943–21960

Bilham R, Behr J (1992) A two layer model for seismic slip on the Superstition Hills Fault, California. BSSA 82(3):1223–1235

Camacho Ibarra EG (2006) Análisis de la deformación vertical del Terreno en la región de Confluencia del Sistemas de Fallas Cerro Prieto—Imperial en el Periodo 1962–2001. Tesís de Maestría, CICESE, p 135

Carnec C, Fabriol H (1999) Monitoring and modeling land subsidence at the Cerro Prieto geothermal field, Baja California, Mexico, using SAR interferometry. Geophys Res Lett 26(9):1211–1214

CFE (2006) Cerro Prieto geothermal field. CFE, Mexico

Chen CW, Zebker HA (2001) Two-dimensional phase unwrapping with use of statistical models for cost functions in nonlinear optimization. J Opt Soc Am A 18:338–351

Contreras J, Martin-Barajas A, Herguera JC (2002) Subsidence and Extensión Rates of Laguna Salada Basin, Northeastern Baja California, Mexico. In: Eos Trans. AGU 83 (47), Fall. Meet. Supll., Abstract T52C–1223, San Francisco

Davis PM (1986) Surface deformation due to inflation of an arbitrary oriented triaxial ellipsoidal cavity in an elastic half-space, with references to Kilauea Volcano, Hawaii. J Geophys Res 91(B7):7429–7438

Fialko Y, Simons M (2000) Deformation and seismicity in the Coso geothermal area, Inyo Country, California: observation and modeling using satellite radar interferometry. J Geophys Res 195(B9):21781–21793

Glowacka E (1996) Major earthquake in Mexicali valley, Mexico, and fluid extraction at Cerro Prieto geothermal field. Bull Seism Soc Am 86:93–105

Glowacka E, Gonzalez J, Fabriol H (1999) Recent vertical deformation in Mexicali Valley and its relationship with tectonics, seismcity and fluid operation in the Cerro Prieto geothermal field. Pure Appl Geophys 156:591–614

Glowacka E, Nava FA, Diaz de Cossio G, Farfán F (2001) Monitoring the response of the imperial fault to fluid extraction in the Cerro Prieto geothermal field, Baja California, Mexico. In: Van Aswegen G, Durrheim RJ, Ortlepp WD (eds) Rockbursts and Seismcity in Mines—RASiM 5, pp 143–147

Glowacka E, Nava FA, Diaz de Cossio G, Wong V, Farfan F (2002) Fault slip, seismicity and deformation in the Mexicali Valley (B.C., Mexico) after the 1999 Hector Mine Earthquake (M = 7.1). Bull Seism Soc Am 92(4):1290–1299

Glowacka E, Sarychikhina O, Nava AF (2005) Subsidence and stress change in the Cerro Prieto geothermal field, B.C., Mexico. Pure Appl Geophys 162:2095–2110

Glowacka E, Sarychikhina O, Suarez F, Mendoza R, Nava F (2006) Estudio geologico para definir la zona de hundimiento con el fin de relocalización del canal Nuevo Delta en el Valle de Mexicali. Reporte Tecnico. CICESE, Mexico, p 505

González JJ, Glowacka E, Suárez F, Quiñónez G, Guzmán M, Castro JM, Riviera F, Félix MG (1998) Movimiento reciente de la falla Imperial, Mexicali, B. C., Divulgare, Ciencia para todos, Mexicali, B. C. 6 (22):4–15

Hanssen RF (2001) Radar interferometry. Kluwer, Netherlands

Johnson NM, Officer CB, Opdyke ND, Woodard GD, Zeitler PK, Lindsay EH (1983) Rates of late Cenozoic Tectonism in the Vallecito–Fish Creek basin. Geology 11:664–667

Kampes B, Hanssen R, Perski Z (2003) Radar interferometry with public domain tools. In: Proceedings of fringe 2003: 1–5 December, Frascati, Italy

King GCP, Stein RS, Lin J (1994) Static stress changes and the triggering of earthquakes. Bull Seismol Soc Am 84(3):935–953

Lippmann MJ, Truesdell AH, Mañón AM, Halfman SE (1991) A review of the hydrogeologic-geochemical model for Cerro Prieto. Geothermics 20:39–52

Lira H (2005) Actualización del modelo geológico conceptual de yacimiento geotérmico de Cerro Prieto, B.C. Geotermia 18:37–46

Lira H, Arellano JF (1997) Resultados de la nivelación de precisión realizada en 1997, en el campo geotérmico Cerro Prieto (Informe técnico RE 07/97, CFE 1997)

Magistrale H (2002) The relation of Southern San Jacinto fault zone to the Imperial and Cerro Prieto faults. Geol Soc Am Special Paper 365:271–178

Mogi K (1958) Relations between the eruptions of various volcanoes and the deformation of the ground surface around them. Bull Earthquake Res Inst Univ Tokyo 36:99–134

Mossop AP, Segall P (1997) Subsidence at the Geysers geothermal field, N. California from a comparison of GPS and leveling surveys. Geophys Res Lett 24:1839–1842

Nava FA, Glowacka E (1999) Fault slip triggering, healing, and viscoelastic afterworking in sediments in the Mexicali_Imperial Valley. Pure Appl Geophys 156:615–629

Ocampo-Diaz J (2005) Cerro Prieto IV, the newest power plant in Cerro Prieto geothermal field. In: Proceedings of thirtieth workshop on geothermal reservoir engineering, Stanford University

Pennington W, Davis SD, Carlson SM, Dupree J, Ewing TE (1986) The evolution of seismic barriers and asperities caused by the depressuring of fault planes in oil and gas of South Texas. BSSA 76(4):939–948

Sarychikhina O (2003) Modelación de subsidencia en el campo geotérmico Cerro Prieto. Tesis de Maestría, CICESE, México

Sarychikhina O, Mellors R, Glowacka E (2007a) Aplication of InSAR to the study of ground deformation in the Mexicali Valley, B.C., MEXICO. In: Proceedings of Envisat symposium, Montreux, Switzerland, p 6. Postsymposium CD

Sarychikhina O, Glowacka E, Mellors R (2007b) Preliminary results of the surface deformation study, using differential InSAR technique at the Cerro Prieto Geothermal Field, B.C., México. GRC meeting, Reno 2007, proceedings CD, pp 581–584

Scharoo R, Visser P (1998) Precise orbit determination and gravity field improvement for the ERS satellites. J Geophys Res 103(C4):8113–8127

Segall P (1989) Earthquakes triggered by fluid extraction. Geology 17:942–946

Sheng Z, Helm DC (1998) Multiple Steps of Earth Fissuring Caused by Ground Water Withdrawal. In: Borchers JW (ed) Tectonic controls of geomorphic processes in land subsidence area. Land Subsidence. Star Publishing Company, pp 149–154

Suarez-Vidal F, Mendoza-Borunda R, Naffarrete-Zamarripa LM, Ramirez J, Glowacka E (2008) Shape and dimensions of the Cerro Prieto pull-apart basin, Mexicali, Baja California, México, based on the regional seismic record and surface structures. Int Geol Rev 50(7):636–649

Talwani P, Acree S (1984/1985) Pore pressure diffusion and the mechanism of reservoir-induced seismicity. Pure Appl Geophys 122:947–965

Toda S, Stein RS, Reasenberg PA, Dieterich JH (1998) Stress transferred by the Mw = 6.9 Kobe, Japan, shock: effect on aftershocks and future earthquake probabilities. J Geophys Res 103:24543–24565

Truesdell AH, Lippmann MJ (1990) Interaction of cold-water aquifers with exploited reservoirs of the Cerro Prieto Geothermal system. Geotherm Resour Counc Trans 14:735–741

Truesdell AH, Lippmann MJ, Gutiérrez PH, de León JV (1998) The Importance of natural fluid recharge to the sustainability of the Cerro Prieto resource. Geotherm Resour Counc Trans 22:529–536

Velasco J (1963) Levantamieno gravimétrico, zona geotérmica de Mexicali, Baja California, Consejo de Recursos Minerales. Technical report, p 55

Wesson RL (1988) Dynamics of fault creep. J Geophys Res 93:8929–8951

Yang X, Davis PM (1986) Deformation due to a rectangular tensional crack in an elastic half-space. Bull Seismol Soc Am 76(3):865–881